European Journal of Pharmacology 688 (2012) 6–13

Contents lists available at SciVerse ScienceDirect

European Journal of Pharmacology

journal homepage: www.elsevier.com/locate/ejphar

Molecular and Cellular Pharmacology

MMPT as a reactive oxygen species generator induces apoptosis via the depletion of intracellular GSH contents in A549 cells

Yun-feng Zhao [a,b,*], Cui Zhang [c], You-rui Suo [b]

[a] School of Life Science, Qufu Normal University, Qufu 273165, PR China
[b] Northwest Institute of Plateau Biology, Chinese Academy of Sciences, Xining 810008, PR China
[c] Department of Biology Science and Technology, Taishan University, Taian 271021, PR China

ARTICLE INFO

Article history:
Received 8 August 2011
Received in revised form 23 April 2012
Accepted 4 May 2012
Available online 17 May 2012

Keywords:
A549 cells apoptosis
Caspase
GSH
MMPT
Reactive oxygen species

ABSTRACT

MMPT, (5-[(4-methylphenyl)methylene]-2-(phenylamino)-4(5H)-thiazolone), a thiazolidin compound, was identified in our laboratory as a novel antineoplastic agent with a broad spectrum of antitumor activity against many human cancer cells. A previous study showed that MMPT inhibited cell growth, and induced apoptosis in H1792 cells. In this study, the antiproliferative activity of MMPT was investigated. The results showed that MMPT was able to inhibit A549 cell growth in a time- and dose-dependent manner by blocking cell cycle progression in the G2 phase and inducing apoptosis. MMPT induced DNA fragmentation and caspase activation in A549 cells, both of which are hallmarks of apoptosis. The apoptotic process was accompanied by the generation of reactive oxygen species, depletion of glutathione (GSH), and reduction the GSH/GSSG ratio, suggesting that MMPT may induce apoptosis in A549 cells through a reactive oxygen species dependent pathway. Treatment with a thiol antioxidant, NAC, showed the recovery of GSH depletion and the reduction of reactive oxygen species levels in MMPT-treated cells, which were accompanied by the inhibition of apoptosis. In contrast, L-buthionine sulfoximine (BSO), a well-known inhibitor of GSH synthesis, aggravated GSH depletion and cell death in MMPT-treated cells. In conclusion, we have demonstrated that MMPT inhibits the growth of A549 cells by inducing a G2 arrest of the cell cycle and by triggering apoptosis accompanied with the depletion of GSH.

1. Introduction

Apoptosis is an important mechanism of controlled cell depletion in response to both physiological and toxic stimuli. Morphologically, apoptosis is characterized by a series of structural changes in dying cells: blebbing of the plasma membrane, cytoplasmic vacuolization, condensation of chromatin, and cellular fragmentation into membrane apoptotic bodies (Cho and Choi, 2002; Wong, 2011). These morphological changes result from the activation of a set of apoptotic signaling pathways. Two well established mechanisms involving apoptotic cell death have been characterized. One is mediated by death receptors, which interact with their ligands including CD95 (Fas/APO-1), TNF-R1, DR3, DR4 (TRAIL-R1), and DR5 (TRAIL-R2) (Falschlehner et al., 2009; Qiao and Wong, 2009). The other is involved in the participation of mitochondria, for most forms of apoptosis in response to cellular stress, loss of survival factors and developmental cues (Ferrín et al., 2011). Recent studies of the endoplasmic reticulum (ER) as a third subcellular compartment containing caspase-4 were implicated in apoptotic execution induced by ER stress (Rasheva and Domingos, 2009; Zhao et al., 2011). Many proteins are involved in this complex process. Central to the apoptotic process are the caspases, a family of cysteine proteases that are activated in a cascade of sequential cleavage reactions from their inactive zymogen precursors (Olsson and Zhivotovsky, 2011; Pop and Salvesen, 2009).

Chemical agents such as anticancer drugs and chemopreventive agents stimulate cells to produce reactive oxygen species (Liu et al., 2009). Generated reactive oxygen species can cause $\Delta\Psi m$ loss by activating mitochondrial permeability transition, and can induce apoptosis by releasing apoptogenic proteins such as cytochrome c to the cytosol (Xu et al., 2012). Reactive oxygen species include hydrogen peroxide (H_2O_2), superoxide anion ($O_2{\bullet}^-$) and hydroxyl radical (•OH). These molecules have recently been implicated in regulating many important cellular events, including transcription factor activation, gene expression, differentiation, and cell proliferation (Cataldi, 2010; Liu et al., 2009; Wolf, 2005). Reactive oxygen species can interact with intracellular macromolecules such as proteins, membrane lipids and nucleic acids. Oxidative attack of proteins can lead to oxidation of amino acid residue side chains, formation of protein–protein cross-linkages, and oxidation of the protein backbone resulting in protein fragmentation (Cataldi, 2010; Wolf, 2005). Cell membrane is another target of reactive oxygen species, and generally the effects of lipid peroxidation are to decrease membrane fluidity, increase the leakiness of the membrane, and inactivate membrane-bound enzymes, leading to complete loss of membrane integrity (Gaetke and

* Corresponding author at: School of Life Science, Qufu Normal University, No. 57, Qufu Jingxuan West Road, Qufu 273165, Shandong Province, PR China. Tel.: +86 537 4456415; fax: +86 537 4456887.
E-mail address: zhaoyf1989@yahoo.com.cn (Y. Zhao).

0014-2999/$ – see front matter © 2012 Elsevier B.V. All rights reserved.
doi:10.1016/j.ejphar.2012.05.003

Chow, 2003; Liu et al., 2009). Cells possess antioxidant systems to control the redox state, which is important for their survival. Excessive production of reactive oxygen species gives rise to the activation of events that lead to death or survival in various cell types (Dasmahapatra et al., 2006; Simon et al., 2000; Wallach-Dayan et al., 2006). GSH is a main non-protein antioxidant in the cell and it can clear away the superoxide anion free radical and provide electrons for enzymes such as glutathione peroxidase, which reduce H_2O_2 to H_2O (Rhee et al., 2005). GSH has been shown to be crucial for regulation of cell proliferation, cell cycle progression and apoptosis (Giannopoulou et al., 2009; Schnelldorfer et al., 2000), and is known to protect cells from toxic insult through detoxification of the toxic metabolites of drugs and reactive oxygen species (Biswas and Rahman, 2009; Lauterburg, 2002).

Although MMPT was demonstrated to induce apoptosis in H1792 human lung cancer cells (Zhao et al., 2010), there is no available information to address MMPT affecting A549 human lung cancer cells and also no information to address the role of reactive oxygen species and GSH on MMPT-induced apoptosis. Therefore, in this study we focused on the mechanism and the role of reactive oxygen species production and GSH depletion on the induction of apoptosis by MMPT in A549 cells.

2. Materials and methods

2.1. Standard cell culture conditions

Human lung cancer cell lines A549 were obtained from American Type Culture Collection (Manassas, VA). Cells were grown in RPMI 1640, supplemented with 10% fetal bovine serum, L-glutamine (2 mM), penicillin (100 units/ml), streptomycin (100 units/ml), and HEPES (25 mM). Normal human lung cells (Wi-38) and normal human fibroblasts cells (NHFB) were maintained in Dulbecco's modified Eagle's medium (DMEM) with the same supplements. All cells were maintained in the presence of 5% CO_2 at 37 °C.

2.2. Chemicals and antibodies

MMPT was synthesized and was structurally confirmed by nuclear magnetic resonance (NMR). The MMPT was dissolved in DMSO to a concentration of 10 mM and stored at 4 °C. Sodium 3′-[1-(phenylamino-carbonyl)-3,4-tetrazolium]-bis(4-methoxy-6-nitro) benzenesulfonic acid hydrate (XTT) was obtained from Roche Diagnostics GmbH (Germany). ApoAlert caspase-3 colorimetric assay kit was purchased from Clontech Laboratories, Inc., (Palo Alto, CA); Nucleosome ELISA was purchased from Calbiochem (Cambridge, MA). L-buthionine sulfoximine (BSO), N-acetylcysteine (NAC), dithiothreitol (DTT), 2,7-dichlorodihydrofluorescein diacetate (DCHFDA), propidium iodide (PI), ribonuclease A (RNase A), Rhodamine 123, and Hoechst 33258 (H33258) were purchased from Sigma Aldrich Chemical (St. Louis, Mo., USA). Fetal bovine serum (FBS), penicillin, streptomycin, RPMI 1640 medium, 4-(2-hydroxyerhyl)-piperazine-1-erhanesulfonicacid (HEPES), and PBS were obtained from GIBCO BRL (Gaithersburg, MD). Monochlorobimane was obtained from Molecular Probes (Eugene, OR). Glutathione kit was obtained from Cayman Chemical (Ann Arbor, MI).

2.3. Cytotoxicity studies

The inhibitory effects of MMPT on cell growth were determined by XTT assay. Briefly, cells were plated in 96-well plates (5×10^3 cells/well). After 24 h incubation the cells were treated with MMPT. The cell viability was determined by XTT assay according to the manufacturer's protocol. Cell viability (%) $= OD_{treatment}/OD_{control}\times100\%$. The IC_{50} value, a dose that causes 50% reduction of surviving cells when compared with control, was determined by the SigmaPlot Version 10.0 program.

2.4. Colony formation assay

The antiproliferative effect of MMPT on A549 cells was assessed by colony formation assay, as described by Roy et al. (2005). Briefly, ~400 cells were plated into each well of 6-well pates in triplicate for 24 h. Thereafter, cells were treated with MMPT. The cells were kept in an incubator at 37 °C for 7 days. On day 8, the colonies were washed with PBS, fixed with formalin (10%), and stained with trypan blue. The colonies that had ≥50 cells per colony were counted. The number of colonies formed in the presence of varying concentrations of MMPT was expressed as a percentage of untreated controls.

2.5. H33258 stained assay

Cells grown on 4-chamber slides were treated with or without MMPT (15 μM) for 48 h. The detection was performed as described previously (Zhao et al., 2010).

2.6. Cell cycle analysis

To determine cell cycle distribution, the cells incubated with MMPT at 15 μM for 12–48 h were harvested by trypsinization, washed with PBS, resuspended in 70% ethanol in PBS, and kept at 4 °C for at least 24 h. Before analysis, the cells were adjusted to a final density of 1×10^6 cells/ml in PBS containing RNase A (1 mg/ml) and stained with 10 mg/ml of PI. The resulting suspension was then passed through a nylon mesh filter and analyzed on a Becton Dickinson FACScan. Cell cycle distribution was calculated using the Modifit-3 program.

2.7. Measurement of apoptosis by ELISA

The induction of apoptosis by MMPT was assayed using the Nucleosome ELISA kit, according to the manufacturer's protocol. The samples of cell lysate were placed in 96-well plates (1×10^6 per well). The induction of apoptosis was evaluated by assessing the enrichment of nucleosome in cytoplasm, and determined exactly as described in the manufacturer's protocol (Salgame et al., 1997).

2.8. Measurement of mitochondrial membrane potential

The mitochondrial membrane potential was determined using the Rhodamine 123 fluorescent dye (from Sigma), a cell-permeable cationic dye that preferentially enters mitochondria based on a highly negative mitochondrial membrane potential ($\Delta\Psi m$). Depolarization of mitochondrial membrane potential ($\Delta\Psi m$) results in the loss of Rhodamine 123 from the mitochondria and a decrease in intracellular fluorescence. In brief, cells were washed twice with PBS and incubated with Rhodamine 123 (0.1 μg/ml) at 37 °C for 30 min. PI (1 μg/ml) was subsequently added, and the staining intensity of Rhodamine 123 and PI was determined by flow cytometry.

2.9. Estimation of intracellular reactive oxygen species

The generation of intracellular reactive oxygen species was measured using DCHFDA (2,7-dichlorodihydrofluorescein diacetate) as the fluorescence probe as described previously (Pandey and Mishra, 2003). Briefly, A549 cells (3×10^5 cells/ml) were incubated with various concentrations of MMPT with respective controls in phosphate buffered saline (PBS) for either 15 or 30 min at 37 °C followed by labeling with the fluorescence probe. Aliquots (200 μl) obtained after different treatments were diluted to 3 ml with PBS followed by measurement of fluorescence intensity using a 490-nm excitation filter and 520-nm emission filter in a FP-6500 Spectrofluorometer (Jasco, Tokyo, Japan).

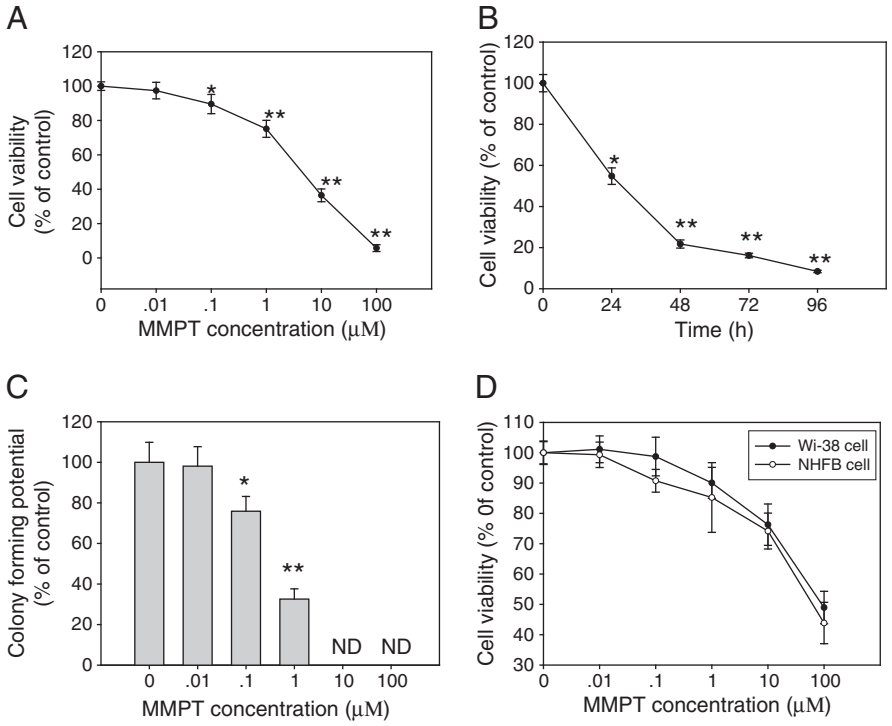

Fig. 1. Effect of MMPT on cell viability in A59, NHFB and Wi-38 cells. (A) A549 cells were treated with the indicated concentrations of MMPT for 48 h and (B) treatment of A549 cells with 15 μM MMPT for the indicated time. The cell viability was assessed by the XTT assay as described in "Materials and methods". A549 cells culture treated with DMSO (control) were taken as 100% of cell viability. (C) Cell proliferation potential and formation were assessed by colony formation assay. *ND*, not detectable. Each data point is a mean of three independent experiments with six wells/concentration and is given as mean ± S.D. *P<0.05, **P<0. 01 vs. DMSO controls (Student's *t*-test). (D) NHFB and Wi-38 cells were treated with various concentrations of MMPT for 48 h, and then their viability was determined by XTT assay. Each data point is a mean of three independent experiments with six wells/concentration and is given as mean ± S.D.

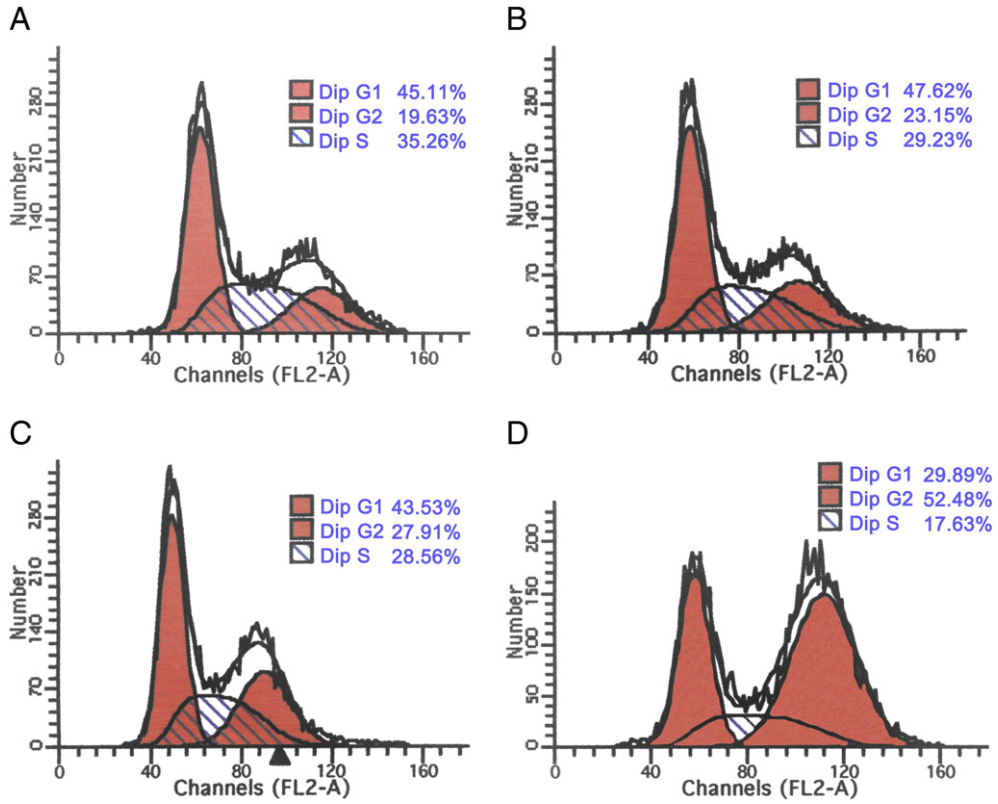

Fig. 2. Effect of TV on cell cycle distribution in A549 cells. A549 cells were treated with or without MMPT 15 μM for 12 h, 24 h, and 48 h, harvested, fixed and stained with PI. The DNA content of the stained cells was analyzed by flow cytometry: (A) DMSO controls, (B) 15 μM MMPT for 12 h, (C) 15 μM MMPT for 24 h and (D) 15 μM MMPT for 48 h. Data are representative of three independent experiments with similar results.

2.10. Determination of glutathione (GSH) and glutathione disulfide (GSSG) levels

Determination of glutathione (GSH) and GSSG levels was determined in A549 cells by glutathione kit obtained from Cayman Chemical (Ann Arbor, MI) as described by us previously (Zhang et al., 2008). Briefly cells were plated at a density of 1×10^6 in 100-mm culture dishes and allowed to attach overnight and treated on the second day with tested agents. Cells were collected by scraping, washed with PBS, and cell lysate was used for determination of GSH level using the above mentioned kit according to the manufacturer's instruction. To determine GSSG levels, GSH was masked by 2-vinyl pyredine for 1 h before the assay. The samples were read at 405 nm at 5 min intervals for 30 min. The GSH and GSSG were evaluated by comparison with standards and normalized with protein content. The results were expressed as total GSH (% of control) or GSH/GSSG ratio, using reduced form GSH or an oxidized form of GSH (GSSG) as the standard.

2.11. Caspase-3 activity assay

Caspase-3 activity in A549 cells was assayed according to the manufacturer's protocol. Briefly, 2×10^6 cells were lysed with lysis buffer and centrifuged at 12,000 rpm at 4 °C for 5 min. Then, the supernatants were mixed with 2× Reaction Buffer containing DTT (10 mM) and caspase-specific substrate, and incubated for 1 h at 37 °C. The samples were read at 405 nm using a micro-plate reader.

2.12. Statistical analysis

Data are expressed as the mean ± standard deviation (S.D.) of three independent experiments, and analyzed by Student's *t*-test. Differences at $P<0.05$ or less were considered statistically significant.

3. Results

3.1. Effect of MMPT on cell proliferation and cell viability

The MMPT that were initially observed to kill A549 cells but not Wi-38 and NHFB underwent two additional screenings to confirm the observation (data not shown). The growth inhibitory effect of MMPT was examined at doses between 0.01 and 100 μM for 48 h. A549 cell growth was markedly inhibited by MMPT treatment in a dose-dependent manner (Fig. 1A), but not Wi-38 and NHFB (Fig. 1D). After 48 h of incubation with 2.8 and 7.5 μM of MMPT, the numbers of viable cells decreased to 70% and 50%, respectively, compared to controls. The effect of MMPT on the cell survival was also time-dependent (Fig. 2B). It is noteworthy that MMPT-mediated reduction of cell viability was dose and time dependent (Fig. 1A and B). Its IC_{50} value was 7.5 μM. Thus, we chose 15 μM MMPT, a concentration close to the IC_{80} value, to detect changes in molecular events in the following experiments.

We also examined the effect of MMPT on the colonogenic survival of A549 cells. There was a drastic decrease in the ability of the A549 cells to form colonies with increasing doses of MMPT (0.1–100 μM) (Fig. 1C). MMPT at dosages of 10 and 100 μM completely inhibited the proliferation of cells with no colonies formed by the end of 7 days. These observations indicated that MMPT has antiproliferative and anticarcinogenic effects on A549 cells.

3.2. Treatment with thiazolidin compounds causes induction of G2/M phase arrest in A549cells

To investigate further features of cell growth inhibition by MMPT, flow cytometric analysis was performed. The results on the effect of MMPT on cell cycle progression of A549 were shown in Fig. 2. The accumulation of cells in the G2/M phase was accompanied by synchronous decreases in the numbers of cells in the G1 and S phases.

3.3. Induction of apoptosis by MMPT

Concomitant with cell growth inhibition induced by MMPT, cell morphological changes were observed using a phase contrast microscope. The cell shrinkage, vacuole and membrane blebbing were observed following MMPT treatment at 15 μM for 48 h (Fig. 3A). The nuclear morphology of dying cells was examined using a fluorescent DNA-binding agent, H33258. A549 cells treated with 15 μM MMPT for 48 h displayed typical morphological features of apoptotic cells, i.e., nucleus condensation and nucleus fragmentation (Fig. 3B).

To confirm the apoptosis induced by MMPT, a Nucleosome ELISA assay was conducted. Fig. 3C shows the time course of DNA fragmentation in continuous treatment with 7.5 and 15 μM of MMPT. DNA fragmentation of A549 cells was found at 12 h and maximized at 48 h after addition of MMPT. In contrast to the control, when cells were treated with MMPT, the number of cells undergoing apoptosis increased about 8.43 and 12.41 fold at 7.5 and 15 μM of MMPT, respectively at 48 h. Based on these results, we demonstrated that MMPT could significantly induce apoptosis of A549 cells in a time-dose-dependent manner.

Morphological assay of apoptosis led us to hypothesize that MMPT might activate the caspase-dependent cell death pathway. Therefore, we examined the effect of MMPT on caspase-3 activation. As can be seen in Fig. 3D and E, MMPT activates caspase 3 in a dose- and time-dependent

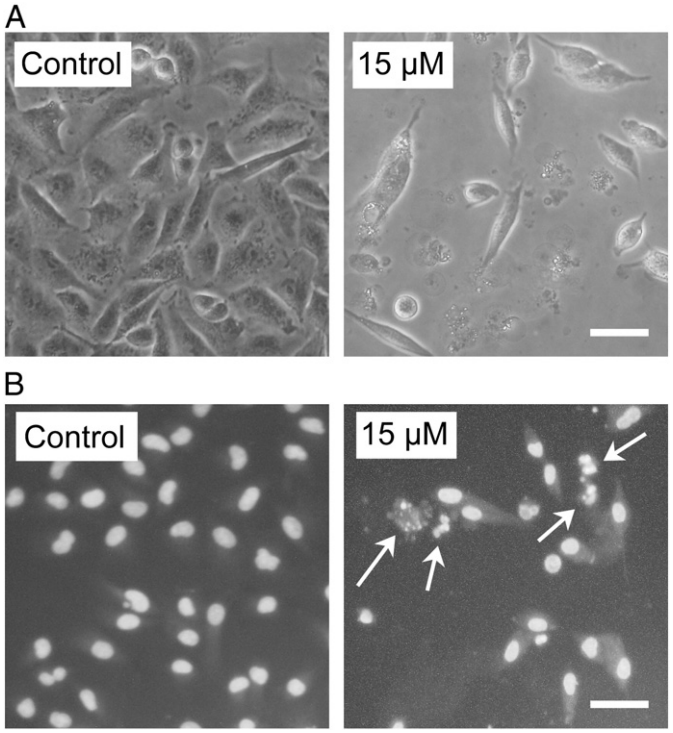

Fig. 3. Effects of MMPT on apoptosis in A549 cells. Exponentially growing cells were treated with the indicated concentrations of MMPT for the indicated times. (A) Morphological changes of A549 cells induced by MMPT. Cells were treated with or without 15 μM MMPT for 48 h, and observed using a phase contrast microscope. Scale bar is 50 μm. (B) Cells were treated with or without 15 μM MMPT for 48 h, stained with H33258, and observed under a fluorescence microscope. Arrows indicate apoptotic nuclei with condensed chromatin. Scale bar is 50 μm. (C) A549 cells were treated with 0, 7.5 μM, and 15 μM of MMPT for 6, 12, 24, and 48 h, respectively. The cell apoptosis was assessed by Nucleosome ELISA. The graph shows the percentages of DNA fragmentation cells. (D) A549 cells were treated with the indicated concentrations of MMPT for 48 h, (E) treatment of A549 cells with 15 μM MMPT for the indicated time, (F) and treatment of A549 cells with the indicated concentration of NAC for 30 min before treating with MMPT (15 μM) for 48 h. Enzymatic activity of caspase 3 was measured. The release of chromophore pNA was monitored spectrophotometrically (405 nm). The data are presented as the mean ± S.D. of the results for three independent experiments. Statistical significance: (C–E) *P<0.05, **P<0.01 vs. DMSO controls. (F) #*P*>0.05, *P<0.05 vs. DMSO controls. **P<0.05 vs. cells treated with MMPT alone (Student's *t*-test).

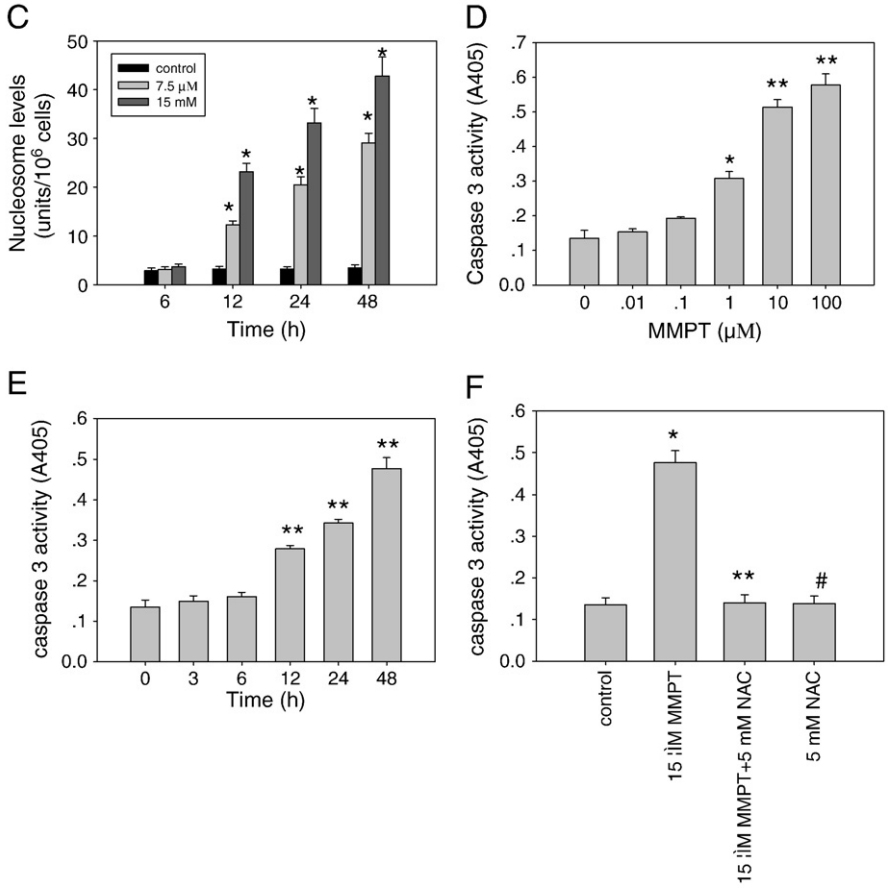

Fig. 3 (*continued*).

manner. This indicated that caspase-3 is involved in the MMPT-induced apoptosis.

3.4. Effects of MMPT on mitochondrial membrane potential (ΔΨm) in A549 cells

To elucidate the effect of MMPT on mitochondrial membrane potential (ΔΨm), cells were treated with the indicated doses of MMPT for the indicated amounts of time (Fig. 4A and B). Treatment with MMPT induced the loss of mitochondrial membrane potential (ΔΨm) in A549 cells in a dose- and time-dependent manner (Fig. 4A and B).

3.5. Effect of MMPT on reactive oxygen species generation and GSH levels in A549 cells

In order to measure the capacity of MMPT to cause intracellular oxidation, we used the specific oxidation-sensitive fluorescent dye DCFH-DA, which leads to an enhanced fluorescent intensity following generation of reactive metabolite intracellular. Fig. 5A shows that MMPT induced a dose dependant increase in reactive oxygen species generation in A549 cells as measured by DCHFDA fluorescent probe.

Reduced GSH is the major non-protein thiol in cells and is essential for maintaining cellular redox status. Since MMPT-induced apoptosis in human lung cancer cells correlated with reactive oxygen species generation, we argued that MMPT treatment might disturb cellular redox status. To address this issue, we determined the effect of MMPT treatment on intracellular GSH levels. MMPT treatment resulted in depletion of intracellular GSH levels in A549 cells in a dose-dependent manner (Fig. 5B). GSH is converted to its oxidized form (GSSG), which must be reduced by the combination of GSH reductase and NADPH. Therefore, an index of cellular oxidative events is the ratio of the levels of the reduced and oxidized forms of GSH. Fig. 5C shows that MMPT induced a dose dependant decrease the ratio of GSH/GSSG in A549 cells. These experiments supported the notion that MMPT treatment affected cellular redox status.

3.6. Effects of NAC and BSO on levels of GSH, apoptosis and reactive oxygen species in MMPT-treated A549 cells

In order to determine whether the observed increase in reactive oxygen species generation and intracellular GSH content had any relevance to MMPT-induced cell death, the effects of the NAC were examined. A549 cells were treated with 5 mM NAC prior to treatment with 15 μM MMPT. As shown in Fig. 6A, the accumulation of reactive oxygen species by MMPT was significantly inhibited by NAC. In addition, NAC inhibited the depletion of GSH content induced by MMPT (Fig. 6B). Next, we examined apoptosis following pretreatment with NAC using the Nucleosome ELISA assay. Fig. 6C shows that pretreatment of A549 cells with NAC protected against MMPT-induced apoptosis. In addition, treatment with NAC significantly reduced the loss of mitochondrial membrane potential ($\Delta\Psi_m$) induced by MMPT (Fig. 4C).

L-buthionine-S,R-sulfoximine (BSO) is an inhibitor of GSH biosynthesis. We investigated whether a decrease in intracellular GSH content is relevant to MMPT-induced cell death in A549 cells. To verify this possibility, A549 cells were treated with 200 μM BSO, prior to treatment with 15 μM MMPT. Treatment with BSO reduced GSH levels in A549 control cells, and intensified the decreased GSH levels in MMPT-treated A549 cells (Fig. 6B). Furthermore, while BSO alone slightly increased reactive oxygen species levels in control cells, it exaggerated reactive oxygen species levels in MMPT-treated cells (Fig. 6A). The GSH levels

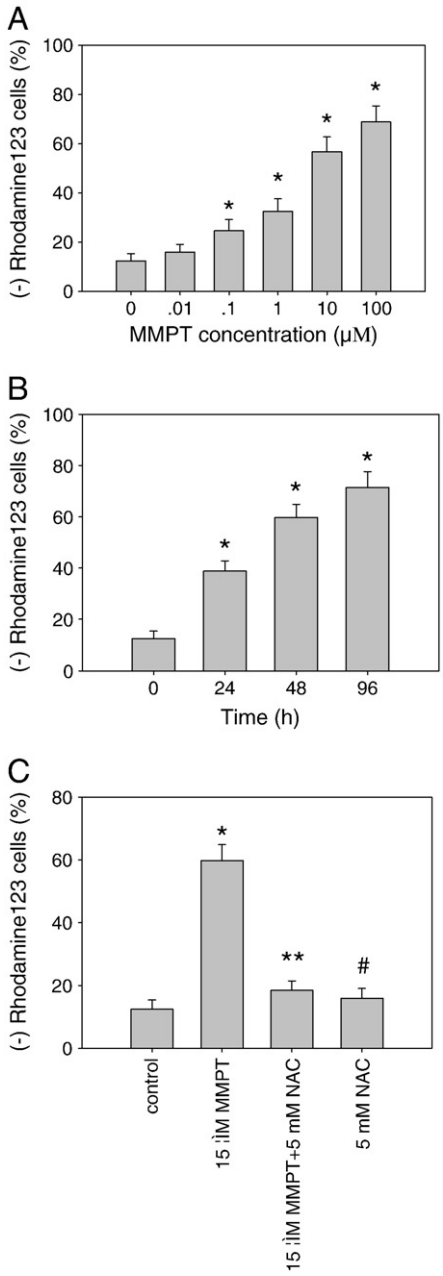

Fig. 4. Effects of MMPT on mitochondrial membrane potential (ΔΨm) in A549 cells. (A) A549 cells were treated with the indicated concentrations of MMPT for 48 h, (B) treatment of A549 cells with 15 μM MMPT for the indicated time, (C) and treatment of A549 cells with the indicated concentration of NAC for 30 min before treating with MMPT (15 μM) for 48 h. Cells were treated with MMPT, stained with Rhodamine 123, and analyzed by flow cytometry. Graph shows the percentages of Rhodamine 123-negative cells. (A,B) *P<0.05 vs. DMSO controls. (C) #P>0.05, *P<0.05 vs. DMSO controls. **P<0.05 vs. cells treated with MMPT alone (Student's *t*-test).

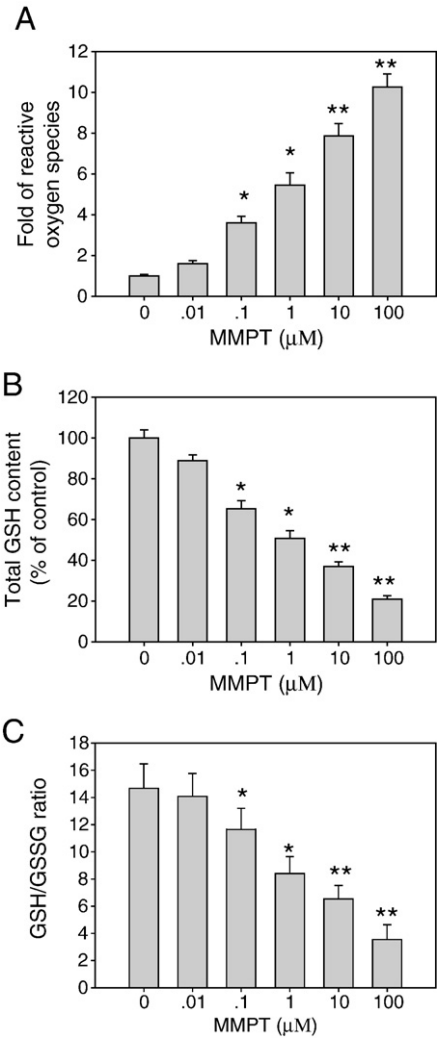

Fig. 5. Effect of MMPT treatment on reactive oxygen species generation, GSH depletion, and GSH/GSSG ratio. (A) Intracellular reactive oxygen species concentration was determined by treating A549 cells with the indicated concentrations of MMPT for 48 h, the cells were loaded with DCFH-DA, and the fluorescence intensity was measured by Fluorescence Spectrometer as described in "Materials and methods". The differences of reactive oxygen species levels in each group were expressed as fold changes. (B) Cells were treated with the indicated concentrations of MMPT for 48 h, and the intracellular GSH content was measured as explained under "Materials and methods". The differences of GSH levels in each group were expressed as % of control. (C) Cells were treated with the indicated concentrations of MMPT for 48 h, and the intracellular GSH content and GSSG level were measured as explained under "Materials and methods". The results were expressed as GSH/GSSG ratio. Each data point is a mean of three independent experiments with 3 dishes/concentration and is given as mean ± S.D. *P<0.05, **P<0. 01 vs. DMSO controls (Student's *t*-test).

reduced by BSO was accompanied with an increase in reactive oxygen species levels. In relation to apoptosis, BSO alone had no significant effect (in view of nucleosome levels), whereas the combined treatment with MMPT and BSO intensified levels of apoptosis in A549 cells (Fig. 6C).

4. Discussion

In the present study, we demonstrated that MMPT decreased the viability of A549 cells in a dose and time-dependent manner. We also have demonstrated that MMPT induced cells cause an arrest in the G2/M phase. MMPT also induced apoptosis at concentrations above 7.5 μM. In the present study, we focused on the mechanisms of MMPT-induced apoptosis in A549 cells in relation to intracellular reactive oxygen species and GSH levels.

Reactive oxygen species are formed as by-products of mitochondrial respiration or precise oxidases including nicotine adenine dephosphate (NADPH) oxidase, xanthine oxidase (XO) and certain arachidonic acid oxygenases (Ling et al., 2003; Viel et al., 2008). And, reactive oxygen species are now thought to be involved in several cellular mechanisms including apoptosis (Cataldi, 2010; Ling et al., 2003). This free radical generation has been shown to accelerate cell death by damaging cellular components, including DNA, proteins, and lipid membranes (Ling et al., 2003; Liu et al., 2009). Studies in a variety of tumor cell types have suggested that cancer chemotherapy drugs induce apoptosis in part by generating endogenous oxidants (Ling et al., 2003; Wolf, 2005). Increasing evidence now demonstrates that the redox status of cells is an important factor in determining whether tumor cells can withstand chemotherapy (Giannopoulou et al., 2009; Wang et al., 2006). Likewise,

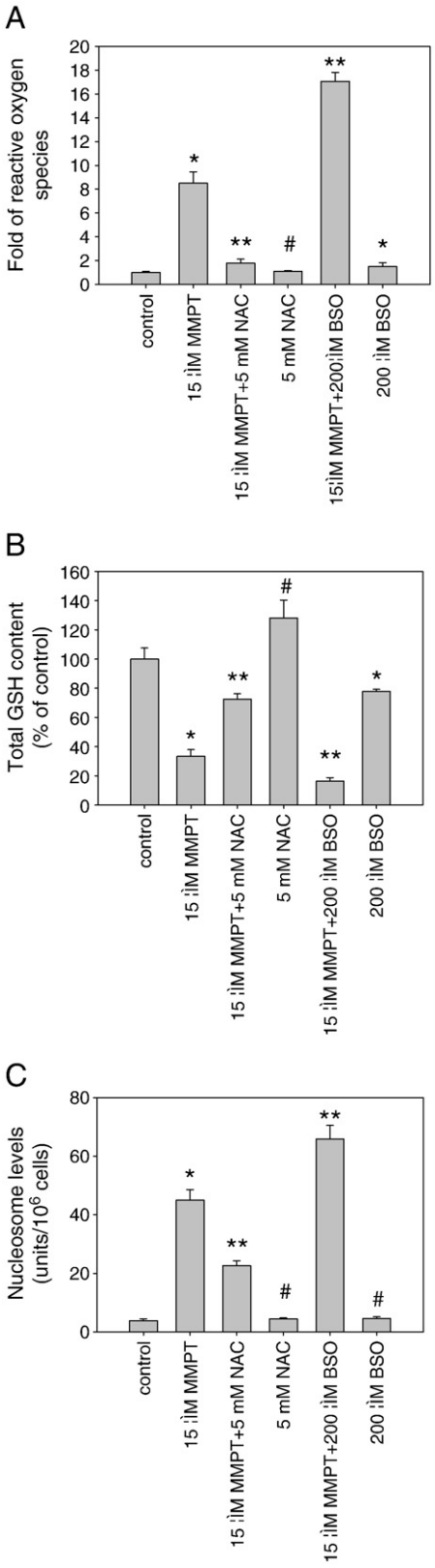

Fig. 6. Effects of NAC and BSO on levels of GSH, apoptosis and reactive oxygen species in MMPT-treated A549 cells. Exponentially growing cells were pretreated with NAC or BSO for 30 min and then exposed to 15 μM of MMPT for 48 h. (A) Intracellular reactive oxygen species levels in cells. (B) Total GSH content in cells. (C) The percent of apoptosis. Each value is the mean ± S.D. of three independent experiments. $^{\#}P > 0.05$, $^{*}P < 0.05$ vs. DMSO controls. $^{**}P < 0.05$ vs. cells treated with MMPT alone (Student's *t*-test).

our data showed that the intracellular reactive oxygen species levels were significantly increased in MMPT-treated A549 cells. Therefore, we investigated whether the intracellular increase in reactive oxygen species levels by MMPT is tightly related to the induction of apoptosis in A549 cells. NAC, like GSH, might enter into the mitochondria, where it plays a protective role as a reactive oxygen species scavenger (Wang et al., 2011). NAC, also an antioxidant, can serve as a precursor to GSH synthesis (Xu et al., 2012). NAC has been shown previously to be thiol antioxidants in drug-induced reactive oxygen species generation, and they inhibit drug-mediated apoptosis (Jung et al., 2005). In our experiment, NAC significantly reduced the level of reactive oxygen species in A549 cells treated with MMPT. This result suggests that the increased cytoplasm GSH by NAC enter the mitochondria to reduce the level of reactive oxygen species in MMPT-treated cells (Kulinsky and Kolesnichenko, 2007). In addition, this decrease was accompanied with the decreased levels of nucleosome cells. The anti-apoptotic effect of NAC was additionally confirmed by attenuation of the activation of caspase-3 (Fig. 3F). These results suggest that the change of intracellular reactive oxygen species by MMPT is at least in part related to apoptosis in A549 cells.

Changes in the intracellular milieu have been reported to be critical for the activation of apoptotic enzymes and the progression of apoptosis (Poh and Pervaiz, 2005; Xu et al., 2012). The GSH has a major role in cellular redox reactions and thiol-ether formation. GSH is a main non-protein antioxidant in the cell, and it can clear away the superoxide anion free radical and provide electrons for enzymes such as glutathione peroxidase, which reduce H_2O_2 to H_2O (Rhee et al., 2005). Reduced GSH is the major non-protein thiol in cells and is essential for maintaining cellular redox status. Intracellular GSH content has a decisive effect on anticancer drug-induced apoptosis, indicating that apoptotic effects are inversely proportional to GSH content (Franco and Cidlowski, 2009; Saha et al., 2009; Sun et al., 2011). Likewise, our results clearly indicated the depletion of intracellular GSH content by MMPT in A549 cells. In addition, pretreatment of A549 cells with BSO, an inhibitor of GSH synthesis, increased the reactive oxygen species levels, and aggravated the GSH depletion and cell death by MMPT. In contrast, thiol-containing compounds such as NAC obviously abated intracellular GSH depletion and blocked the cell death induced by MMPT. These results support that intracellular GSH levels are tightly related to MMPT-induced cell death.

In our previous study, we have demonstrated that MMPT induced growth inhibition of H1792 cells through Fas-mediated and caspase-dependent apoptosis pathway, which suggested that MMPT might be used as a Fas/FasL and caspases promoter to initiate lung cancer cell apoptosis. Then, we determined the relationship of MMPT-induced apoptosis and intracellular oxidation in H1792 cells. But the intracellular reactive oxygen species and GSH levels were not changed in the MMPT-induced cell death of H1792 cells (data not shown). This result is not consistent with present study, which indicated that increased reactive oxygen species and depletion of GSH played an important role in MMPT-induced cell death in A549 cells.

In summary, MMPT inhibited the growth of A549 cells by inducing a G2 arrest of the cell cycle and by triggering apoptosis. The induction of apoptosis by MMPT is accompanied by the activation of caspase-3, and is mostly prevented by inhibitors of caspase. Our study also demonstrated that MMPT induced oxidative stress by increasing reactive oxygen species levels in A549 cells and depletion of intracellular GSH. In conclusion, our data suggested that MMPT, as a reactive oxygen species generator, inhibits the growth of A549 cells by inducing a G2 arrest of the cell cycle, and induces apoptosis via the depletion of GSH contents in A549 cells.

Acknowledgments

We thank journalist Bradford J.A. Franklin for the careful English revision. This project was supported by the Natural Science Foundation of Shandong Province (Y2008D05), Doctoral Foundation of Shandong

Province (BS2011SF006) and the 12th Five-year Plan Provincial Key Construction of Qufu Normal University.

References

Biswas, S.K., Rahman, I., 2009. Environmental toxicity, redox signaling and lung inflammation: the role of glutathione. Mol. Aspects Med. 30, 60–76.

Cataldi, A., 2010. Cell responses to oxidative stressors. Curr. Pharm. Des. 12, 1387–1395.

Cho, S.G., Choi, E.J., 2002. Apoptotic signaling pathways: caspases and stress-activated protein kinases. J. Biochem. Mol. Biol. 35, 24–27.

Dasmahapatra, G., Rahmani, M., Dent, P., Grant, S., 2006. The tyrphostin adaphostin interacts synergistically with proteasome inhibitors to induce apoptosis in human leukemia cells through a reactive oxygen species (ROS)-dependent mechanism. Blood 107, 232–240.

Falschlehner, C., Ganten, T.M., Koschny, R., Schaefer, U., Walczak, H., 2009. TRAIL and other TRAIL receptor agonists as novel cancer therapeutics. Adv. Exp. Med. Biol. 647, 195–206.

Ferrín, G., Linares, C.I., Muntané, J., 2011. Mitochondrial drug targets in cell death and cancer. Curr. Pharm. Des. 17, 2002–2016.

Franco, R., Cidlowski, J.A., 2009. Apoptosis and glutathione: beyond an antioxidant. Cell Death Differ. 16, 1303–1314.

Gaetke, L.M., Chow, C.K., 2003. Copper toxicity, oxidative stress, and antioxidant nutrients. Toxicology 189, 147–163.

Giannopoulou, E., Antonacopoulou, A., Matsouka, P., Kalofonos, H.P., 2009. Autophagy: novel action of panitumumab in colon cancer. Anticancer Res. 29, 5077–5082.

Jung, E.M., Lim, J.H., Lee, T.J., Park, J.W., Choi, K.S., Kwon, T.K., 2005. Curcumin sensitizes tumor necrosis factor-related apoptosis-inducing ligand (TRAIL)-induced apoptosis through reactive oxygen species-mediated upregulation of death receptor 5 (DR5). Carcinogenesis 26, 1905–1913.

Kulinsky, V.I., Kolesnichenko, L.S., 2007. Mitochondrial glutathione. Biochemistry (Mosc.) 72, 698–701.

Lauterburg, B.H., 2002. Analgesics and glutathione. Am. J. Ther. 9, 225–233.

Ling, Y.H., Liebes, L., Zou, Y., Perez-Soler, R., 2003. Reactive oxygen species generation and mitochondrial dysfunction in the apoptotic response to bortezomib, a novel proteasome inhibitor, in human h460 non-small cell lung cancer cells. J. Biol. Chem. 278, 33714–33723.

Liu, C.Y., Lee, C.F., Wei, Y.H., 2009. Role of reactive oxygen species-elicited apoptosis in the pathophysiology of mitochondrial and neurodegenerative diseases associated with mitochondrial DNA mutations. J. Formos. Med. Assoc. 108, 599–611.

Olsson, M., Zhivotovsky, B., 2011. Caspases and cancer. Cell Death Differ. 18, 1441–1449.

Pandey, B.N., Mishra, K.P., 2003. In vitro studies on radiation induced membrane oxidative damage in apoptotic death in mouse thymocytes. Int. J. Low Radiat. 1, 113–119.

Poh, T.W., Pervaiz, S., 2005. LY294002 and LY303511 sensitize tumor cells to drug-induced apoptosis via intracellular hydrogen peroxide production independent of the phosphoinositide 3-kinase-Akt pathway. Cancer Res. 65, 6264–6274.

Pop, C., Salvesen, G.S., 2009. Human caspases: activation, specificity, and regulation. J. Biol. Chem. 284, 21777–21781.

Qiao, L., Wong, B.C., 2009. Targeting apoptosis as an approach for gastrointestinal cancer therapy. Drug Resist. Updat. 12, 55–64.

Rasheva, V.I., Domingos, P.M., 2009. Cellular responses to endoplasmic reticulum stress and apoptosis. Apoptosis 14, 996–1007.

Rhee, S.G., Yang, K.S., Kang, S.W., Woo, H.A., Chang, T.S., 2005. Controlled elimination of intracellular $H_{(2)}O_{(2)}$: regulation of peroxiredoxin, catalase, and glutathione peroxidase via post-translational modification. Antioxid. Redox Signal. 7, 619–626.

Roy, A.M., Baliga, M.S., Katiyar, S.K., 2005. Epigallocatechin-3-gallate induces apoptosis in estrogen receptor-negative human breast carcinoma cells via modulation in protein expression of p53 and Bax and caspase-3 activation. Mol. Cancer Ther. 4, 81–90.

Saha, B., Mukherjee, A., Samanta, S., Saha, P., Ghosh, A.K., Santra, C.R., Karmakar, P., 2009. Caffeine augments Alprazolam induced cytotoxicity in human cell lines. Toxicol. In Vitro 23, 1100–1109.

Salgame, P., Varadhachary, A.S., Primiano, L.L., Fincke, J.E., Muller, S., Monestier, M., 1997. An ELISA for detection of apoptosis. Nucleic Acids Res. 25, 680–681.

Schnelldorfer, T., Gansauge, S., Gansauge, F., Schlosser, S., Beger, H.G., Nussler, A.K., 2000. Glutathione depletion causes cell growth inhibition and enhanced apoptosis in pancreatic cancer cells. Cancer 89, 1440–1447.

Simon, H.U., Haj-Yehia, A., Levi-Schaffer, F., 2000. Role of reactive oxygen species (ROS) in apoptosis induction. Apoptosis 5, 415–418.

Sun, Y., Huang, L., Mackenzie, G.G., Rigas, B., 2011. Oxidative stress mediates through apoptosis the anticancer effect of phospho-nonsteroidal anti-inflammatory drugs: implications for the role of oxidative stress in the action of anticancer agents. J. Pharmacol. Exp. Ther. 338, 775–783.

Viel, E.C., Benkirane, K., Javeshghani, D., Touyz, R.M., Schiffrin, E.L., 2008. Xanthine oxidase and mitochondria contribute to vascular superoxide anion generation in DOCA-salt hypertensive rats. Am. J. Physiol. Heart Circ. Physiol. 295, H281–H288.

Wallach-Dayan, S.B., Izbicki, G., Cohen, P.Y., Gerstl-Golan, R., Fine, A., Breuer, R., 2006. Bleomycin initiates apoptosis of lung epithelial cells by ROS but not by Fas/FasL pathway. Am. J. Physiol. 290, 790–796.

Wang, X.J., Hayes, J.D., Wolf, C.R., 2006. Generation of a stable antioxidant response element-driven reporter gene cell line and its use to show redox-dependent activation of nrf2 by cancer chemotherapeutic agents. Cancer Res. 66, 10983–10994.

Wang, J., Wang, H., Hao, P., Xue, L., Wei, S., Zhang, Y., Chen, Y., 2011. Inhibition of aldehyde dehydrogenase 2 by oxidative stress is associated with cardiac dysfunction in diabetic rats. Mol. Med. 17, 172–179.

Wolf, G., 2005. Role of reactive oxygen species in angiotensin II-mediated renal growth, differentiation, and apoptosis. Antioxid. Redox Signal. 7, 1337–1345.

Wong, R.S., 2011. Apoptosis in cancer: from pathogenesis to treatment. J. Exp. Clin. Cancer Res. 30, 87–100.

Xu, H.L., Yu, X.F., Qu, S.C., Qu, X.R., Jiang, Y.F., Sui, D.Y., 2012. Juglone, from Juglans mandshruica Maxim, inhibits growth and induces apoptosis in human leukemia cell HL-60 through a reactive oxygen species-dependent mechanism. Food Chem. Toxicol. 50, 590–596.

Zhang, R., Humphreys, I., Sahu, R.P., Shi, Y., Srivastava, S.K., 2008. In vitro and in vivo induction of apoptosis by capsaicin in pancreatic cancer cells is mediated through ROS generation and mitochondrial death pathway. Apoptosis 13, 1465–1478.

Zhao, Y.F., Li, X.L., Sun, Y.X., Niu, W., Hu, Z.L., 2010. MMPT: a thiazolidin compound inhibits the growth of lung cancer H1792 cells via Fas-mediated and caspase-dependent apoptosis pathway. Invest. New Drugs 28, 318–325.

Zhao, Y., Zhu, C., Li, X., Zhang, Z., Yuan, Y., Ni, Y., Liu, T., Deng, S., Zhao, J., Wang, Y., 2011. Asterosaponin 1 induces endoplasmic reticulum stress-associated apoptosis in A549 human lung cancer cells. Oncol. Rep. 26, 919–924.